3.1Introduction

The present chapter is a detailed discussion of the synthesis method for preparation of reduced graphene oxide-ZnO nano-composites (rGO-ZnO). In this section, the materials utilized for the synthesis of composites are also discussed and mentioned in different tables form. Works on the synthesis of rGO-ZnO also were showed as a flowchart diagram. Finally, the characterizations techniques were used for rGO-ZnO nano-composite also discussed.

3.2 Materials

In the synthesis, all materials are used as an analytical grade, and it is not further purified.

3.2.1 Materials for synthesis of graphene oxide

For the synthesis of graphene oxide, the requirement of materials, their purity and manufacturing company name were listed in table 3.1.

Table-3.1 Materials for synthesis of graphene oxide

Chemical	Purity (%)	Manufacturing Com. Name
Pyrolytic graphite	99%	Bay Carbon
$KMnO_4$	99%	Loba Chemie
H_2SO_4	98%	Loba Chemie
H_3PO_4	85%	Loba Chemie
$NaNO_3$	98%	Loba Chemie
H_2O_2	30%	Loba Chemie

3.2.2 Pyrolytic Graphite Powder

Pyrolytic graphite (PG) is carbonic materials. It is a form of graphite. The product of pyrolytic graphite was manufactured by decomposition of a hydrocarbon gas at very high temperature in a vacuum furnace. Pyrolytic graphite product obtained by this method is high quality. The physical properties of pyrolytic graphite (PG) are listed in table 3.2, and their powder image is shown in figure 3.1.

Table 3.2 The physical properties of pyrolytic graphite.

Physical Properties	Properties
Surface area	(874 $m^2 g^{-1}$)
Fixed carbon	99%
Particles size	<50μm
Density ρ	2.18-2.2g/cm^3 at 20 ^{0}C
Interplaner distance	<1A^0

Figure 3.1 Pyrolytic Graphite Powder.

3.2.3 Potassium Permanganate ($KMnO_4$)

The chemical formula of potassium permanganate is $KMnO_4$. It is an inorganic chemical compound and its salt consisting of K^+ and MnO_4^- ions which give strong oxidation. Water is the best medium for its dissolution, which provides a pink or purple solution the powder image of $KMnO_4$ shown in figure 3.2.

Figure 3.2 Potassium Permanganate.

3.2.4 Sulphuric acid (H_2SO_4)

Sulphuric acid is colorless. It consists of sulphur, oxygen, and hydrogen, with the molecular formula (H_2SO_4). It is highly exothermic, corrosive materials. It is soluble in water.

3.2.5 Phosphoric acid (H_3PO_4)

Phosphoric acid is also known as ortho-phosphoric acid. The chemical formula of Phosphoric acid is (H_3PO_4). It is non-toxic acid, and its conjugate base is the hydrogen phosphate ion, H_2PO-.

3.2.6 Sodium nitrate ($NaNO_3$)

Sodium nitrate is a white solid material. The chemical formula of sodium nitrate is $NaNO_3$. It is soluble in water. It is used as an industrial scale for the production of fertilizers etc. because it was having nitrate anion (NO_3^-). The powder image of $NaNO_3$ shown in figure 3.3.

Figure 3.3 Sodium nitrate powders.

3.2.7 Hydrogen peroxide (H_2O_2)

Hydrogen peroxide consists of hydrogen and oxygen. The chemical formula of hydrogen peroxide is H_2O_2. It is a very pale blue when it is in pure form.

3.3 Materials for synthesis of Zinc Oxide

For the synthesis of Zinc Oxide, the materials required, their purity and manufacturing company name are listed in table 3.3.

Table-3.3 Materials for synthesis of ZnO nanoparticles.

Chemical	Purity (%)	Manufacturing Com. Name
$ZnSO_4.7H_2O$	99%	Sigma-Aldrich
NaOH	98%	Loba Chemie
Ammonia Solution	100%	Loba Chemie
Deionized water	100%	Loba Chemie

3.3.1 Zinc Sulfate Heptahydrate ($ZnSO_4 \cdot 7H_2O$)

Zinc sulfate is consisting of zinc sulfate ($ZnSO_4$) as well as any of three hydrates. It is inorganic compound with formula $ZnSO_4 \cdot 7H_2O$.Zinc Sulfate Heptahydrate is a colorless solid material that is a common source of soluble zinc ions. It is in powder form and is an eye irritant. At low temperature, it is not converted into zinc sulfate and water. When $ZnSO_4 \cdot 7H_2O$ was heated at 280^0C, it gets converted into zinc sulfate and water by thermal decomposition (StraszkoJ. et al.1997) according to the following equation.

ZnSO4.7H2O →ZnSO4.6H2O+H2O---------- (3.1)

ZnSO4.6H2O →ZnSO4.H2O +5H2O---------- (3.2)

ZnSO4.H2O →ZnSO4+H2O---------- (3.4)

3.3.2 Sodium hydroxide (NaOH)

Sodium hydroxide (NaOH) is a white crystalline solid material at room temperature and absorbs moisture from the air. It is also known as caustic soda. When NaOH dissolved in water or neutralized with acid, it releases substantial amounts of heat, which may prove sufficient to ignite combustible materials. Sodium hydroxide is highly corrosive.

3.3.3 Ammonium hydroxide

Ammonium hydroxide is a solution of ammonia in water. It is also known as ammonia, aqueous ammonia. It is denoted by the symbols NH_3 (aq). Although it suggests an alkali with composition [NH4+][OH-], it is impossible to isolate samples of NH_4OH. The ions NH_4^+ and OH^- do not account for a significant fraction of the total amount of ammonia except in extremely dilute solution.

3.4 Synthesis

The synthesis method of reduced graphene oxide and its composites with ZnO is described in the below section.

3.4.1 Preparation of reduced graphene oxide

Reduced graphene oxide (rGO) was prepared by using the modified Hummers Hoffman method (Hummers W.S., Offeman R. E. 1958). In this method, graphite powder was used as the starting material, and a mixture of concentrated H_2SO_4 and H_3PO_4 in the volume ratio of 9:1 was used. Then the combination of H_2SO_4 and H_3PO_4 was cooled in an ice bath before taking it into use and taking the 120ml of the ice-cooled acidic mixture in a beaker. In this, the concentration of 2.5g

of graphite powder and 2.5g of $NaNO_3$ were aliquot added. The solution of these mixtures was magnetically stirred in a continuous mode. When this adequate dispersion was observed, then 15g of $KMnO_4$ was added in the suspension in an aliquot manner, and the suspension was vigorously stirred. In the next step, the suspension was kept in the ice bath, and it was allowed for reactions for at least two hours. The suspension was taken out from the ice bath, and it was further stirred for another two hours in a preheated water bath while maintaining the temperature in the range of 35-40^{0}C. Finally, the suspension was allowed to cool, and also it was kept in an ice bath. In this stage, deionized water was added to maintain the volume of 400ml. The precipitate was washed with deionized water and then thoroughly dried in an oven. The typical synthesis scheme of GO was shown in figure.3.4.

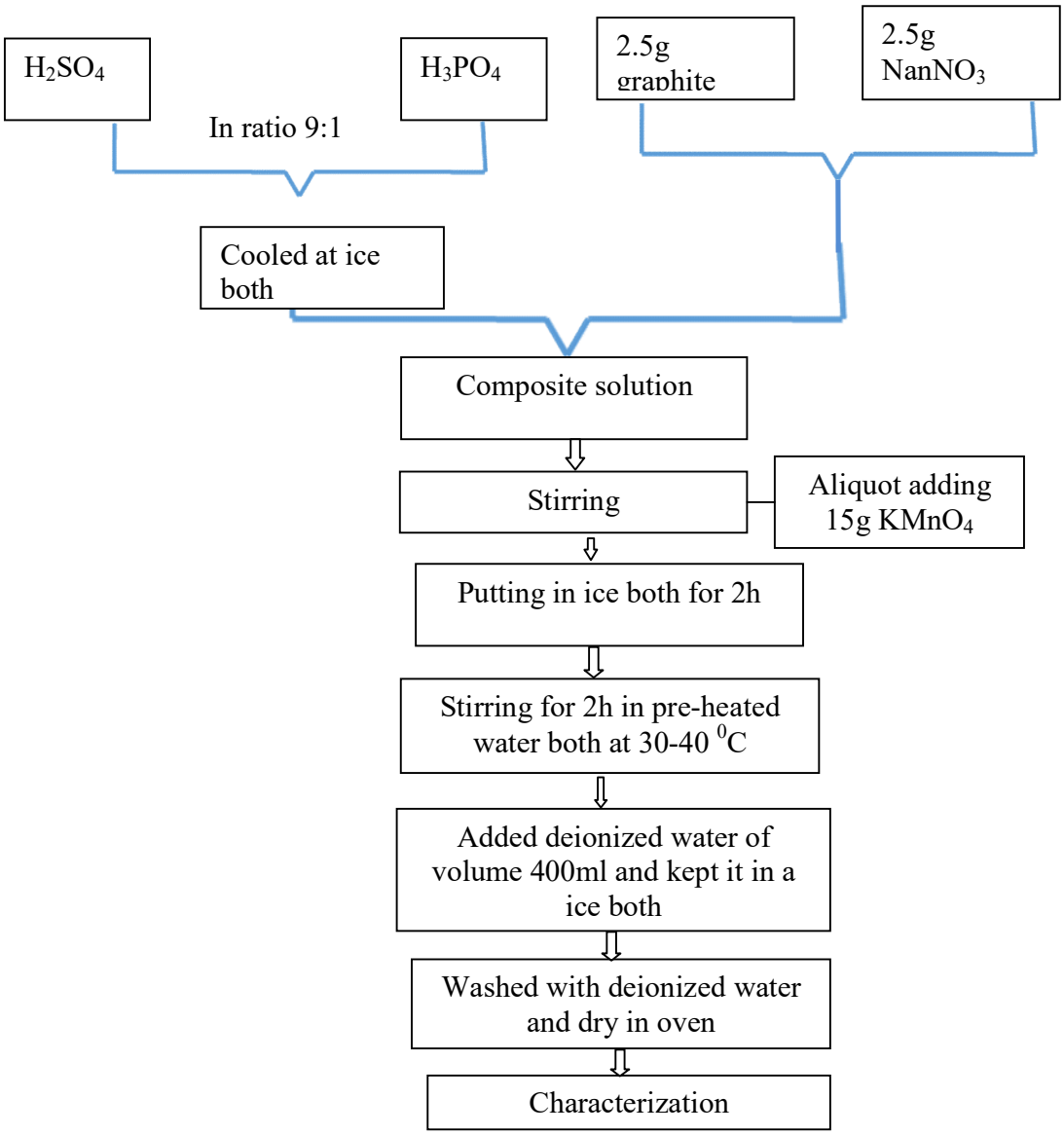

Figure 3.4 Synthesis process of reduced graphene oxide.

3.4.2 Preparation of lotus like ZnO-rGO nano-ceramic composite by sol-gel method

The reduced graphene oxide was synthesized by the previous method, as discussed in section (3.4.1). Reduced graphene oxide-ZnO nano-composite (rGO-ZnO) was synthesized by sol-gel method. For the preparation of salt solutions, deionized water was used. The similar DI water was also used for washing the precipitates. In the first step, GO was prepared by the previous method, as discussed in section (3.4.1). In the second step, 0.01M solution of $ZnSO_4.7H_2O$ (in deionized water) was prepared. The solution was stirred on a magnetic stirrer to obtain a clear solution. It was further heated in a controlled temperature electric oven at 280^0C for thermal decomposition to produce zinc sulfate and water. Then, dilute ammonia solution slowly added drop-by-drop at room temperature, and sonicated solution of GO with a concentration of 0.01mg/ml was added to this solution. After this, the composite solution was stirred, and the temperature of each sample maintained at 60^0C, 70^0C, 80^0C, 90^0C and 100^0C respectively. These were in turn named as RZ60, RZ70, RZ80, RZ90 and RZ100. Here RZ is denoted to reduced graphene oxide and zinc composites. Each sample was centrifuged at 2500rpm for 30min. After the centrifuging, the precipitate was removed and washed with deionized water. It was put in the vacuum oven overnight for drying. The dried precipitates were grinded to a fine powder for further characterizations. The samples of RZ60 and RZ100 were also characterized by SEM. The typical synthesis scheme of rGO-ZnO composite was shown in figure.3.5.

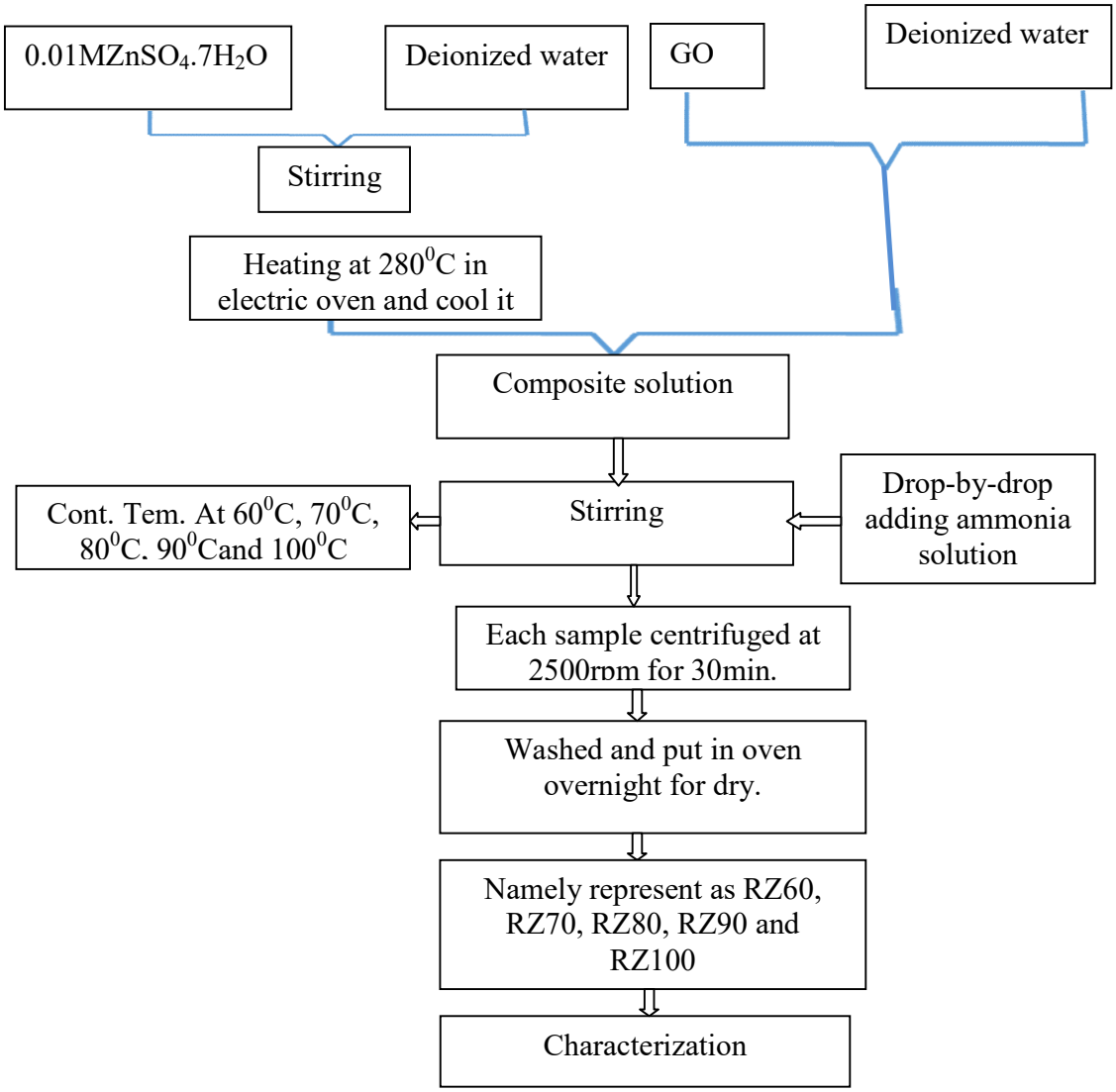

Figure 3.5 Synthesis process of lotus- like ZnO with rGO nanoceramic composites.

3.4.3 Preparation of columnar shaped ZnO-rGO nanoceramic composite by two-step method

For the preparation of columnar shaped ZnO with rGO, the concentrations of GO were selected as 0.01mg/ml, 0.03mg/ml, and 0.05mg/ml which preparation method discussed in section (3.4.1). These Go concentrations were added separately in ethanol with continuous stirring in a beaker at room temperature. In another beaker 50ml of 0.05M $ZnSO_4.7H_2O$ was taken. These two solutions were mixed, and then in this mixed solution, NaOH (0.05M) was added drop-by-drop with constant stirring and maintaining pH~6, (acidic condition) to 9 and 12 (alkaline condition). The samples were coded as RZ-pH6, RZ-pH9, RZ-pH12, respectively. Here RZ is denoted to reduced graphene oxide and zinc composites. Each sample was centrifuged at 3000rpm for 30min. The precipitate was removed from the centrifuge then washed with dilute HCl and finally with deionized water. The precipitates were dried at a constant temperature of 90^0C for at least twenty-four hours in an electric oven. The completely dried precipitates were grinded and then sieved with the 37μm sieve. The typical synthesis scheme of rGO-ZnO composite was shown in figure.3.6.

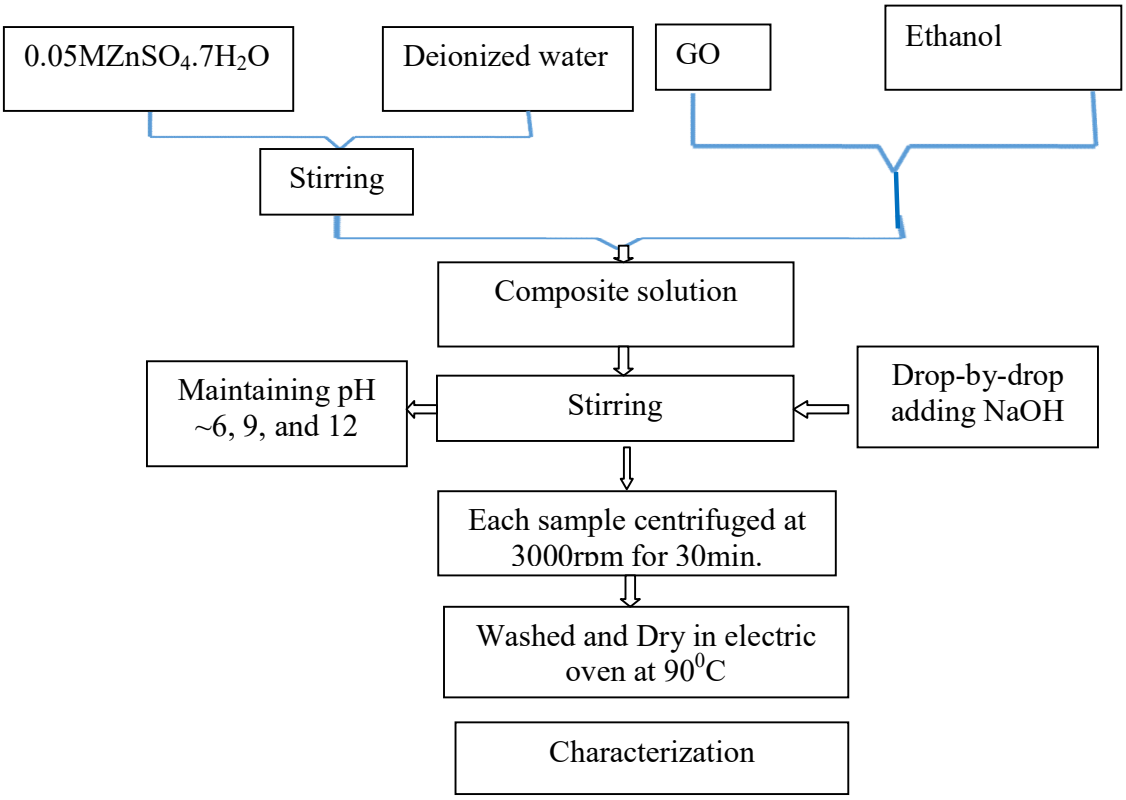

Figure 3.6 Synthesis process of Columnar shaped ZnO with rGO nanoceramic composites.

Furthermore, to optimize the experimental conditions for the preparation of columnar shaped ZnO and lotus-like ZnO with rGO nanoceramic composites, numerous samples with different parameters were synthesized, as listed in table 3.4 and 3.5.

3.4.4 Synthesis of hexagonal Zinc oxide Nanoparticles by sol-gel method

ZnO hexagonal nanoparticles were synthesized by sol-gel method using ammonia as a precursor. In the typical scheme of synthesis shown in figure.1 in which 0.5M $ZnSO_4.7H_2O$ was dissolved in 200ml of distilled water, and it was kept under constant stirring for 30min to complete dissolution. Ammonia solution was acted as a precipitating agent and added drop-wise into $ZnSO_4.7H_2O$ solution with

vigorous stirring. Then the mixture was placed on a hot plate at 85^0C for 2hr to allow complete growth of nanoparticles. The final precipitating solution was turned to whitish cloudy. The white precursor product was centrifuged at 8000rpm for 10min and washed with distilled water to remove impurities or possible absorbed ions. The obtained product was annealed at 700^0C, 900^0C, and 1100^0C for 5h with constant heating rates using muffle furnace. Each sample, namely represented by ZnO700, ZnO900, and ZnO1100, respectively. The annealed samples were then allowed to cool down at room temperature prior to further characterization. The typical synthesis scheme of hexagonal Zinc oxide Nanoparticle was shown in figure.3.7.

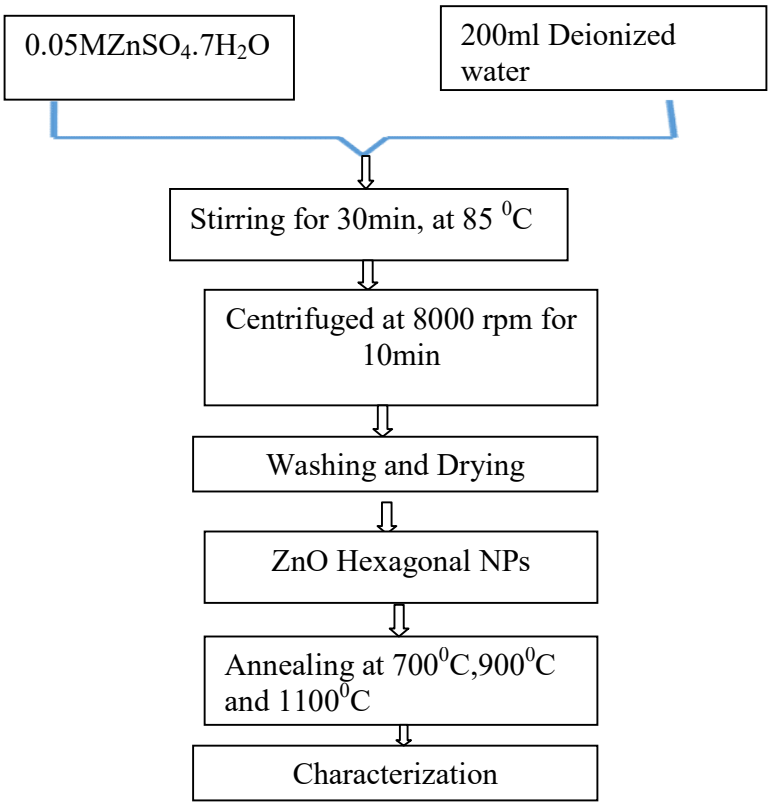

Figure 3.7 Synthesis of hexagonal Zinc oxide Nanoparticles.

3.4 Experimental conditions

3.4.1 Experimental conditions for lotus like ZnO-rGO

Experimental conditions for the preparation of lotus like ZnO nano-ceramics with rGO are different and were listed in table 3.4.

Table 3.4 Different experimental condition of lotus like ZnO-rGO

Sample code	Temperature (0C)	rGOWt%
RZ60	60	0.01
RZ70	70	0.01
RZ80	80	0.01
RZ90	90	0.01
RZ100	100	0.01

3.4.2 Experimental conditions for columnar shaped ZnO-rGO

Experimental conditions for the preparation of columnar shaped ZnO with rGO are different and were listed in table 3.5

Table 3.5 Different experimental condition of columnar like ZnO-rGO

Sample code	pH value	rGOWt%
RZ-PH6	6	0.01
RZ-PH9	9	0.03
RZ-PH12	12	0.05

3.4.3 Experimental conditions for ZnO hexagonal nanoparticles

Experimental conditions for the preparation of ZnO hexagonal nanoparticles are different and were listedin table 3.6

Table 3.6 Different experimental condition of ZnO hexagonal nanoparticles

Sample code	Annealing Temperature(^{0}C)
ZnO	Room Tem.
ZnO700	700
ZnO900	900
ZnO1100	1100

3.5 Experimental Technique

3.5.1 Photocatalytic activity measurement experiment for phenolic compound

Photocatalytic activity was performed by using composites RZ70, RZ80 and RZ90 as the catalyst under sunlight irradiation. The catalyst RZ70, RZ80, and RZ90 with concentration 0.1mg/ml was added to the solution of 0.01M phenol respectively. The mixtures of these two solutions were sonicated to obtain a clear solution. The mixture reaction was placed on a magnetic stirring plate in a closed box under the dark condition for 1h to reach absorption/desorption equilibrium. When natural sunlight exposed on the sample, the presence of phenol in solution will vaporize. For the All samples are covered with thin transparent sheet (Dura seal) to stop the evaporation process of phenol present in the solution when irradiated with sunlight. The mixture was then put under natural sunlight exposure for 00 min, 05min, 10min, 15min and 20min in the summer season. However, the concentration of 0.01M

phenol is used before being exposed to the sunlight. In each cyclic process, the catalyst was tested with the fresh solution of 0.01M phenol and recollected after washing and further used in the photocatalytic experiment. The schematic diagram for measurement of degradation of Phenolic compound was shown in figure 3.8.

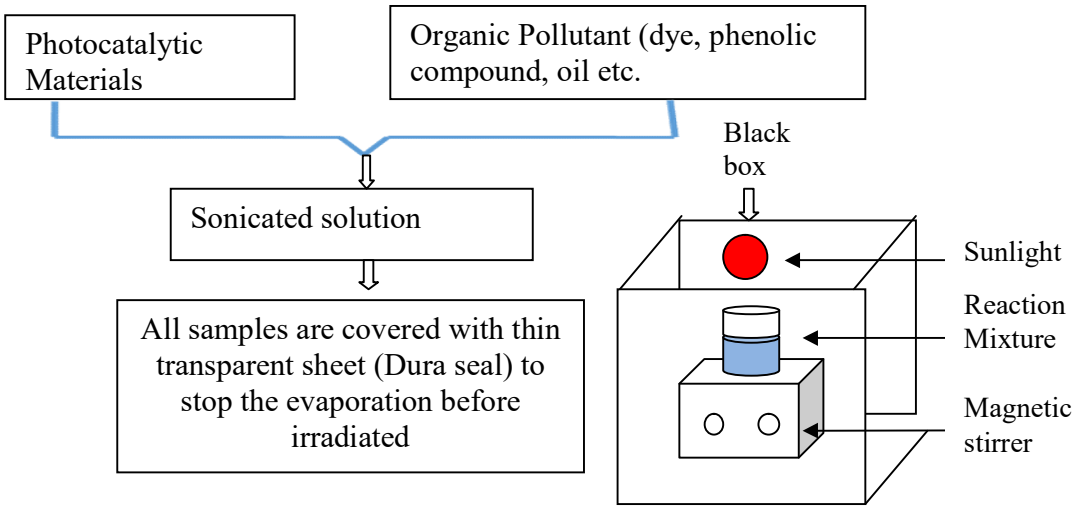

Figure 3.8 Schematic diagrams for photocatalytic activity measurement of phenolic compound.

The degradation rate of phenol is expressed as the following relation:

$D=(C_0-C_t/C_0)\ x100$----------(3.5)

Where C_0 is initial concentration C_t is final concentration

3.5.2 Photocatalytic activity measurement experiment for natural dye

The photocatalytic activity was performed by using composites RZ70, RZ80, and RZ90 as the catalyst under sunlight irradiation. The catalyst RZ70, RZ80, and RZ90 with concentration 0.1mg/ml were added to the solution of 0.01M phenol, respectively. The mixtures of these two solutions were sonicated to obtain a clear solution. The mixture reaction was placed on a magnetic stirring plate in a closed box

under the dark condition for 1h to reach absorption/desorption equilibrium. When natural sunlight exposed to the sample, the presence of phenol in solution will vaporize. For the All samples are covered with a thin transparent sheet (Dura seal) to stop the evaporation process of phenol present in the solution when irradiated with sunlight. The mixture was then put under natural sunlight exposure for 00 min, 05min, 10min, 15min and 20min in the summer season. However, the concentration of 0.01M phenol is used before being exposed to the sunlight. In each cyclic process, the catalyst was tested with the fresh solution of 0.01M phenol and recollected after washing and further used in the photocatalytic experiment. The schematic diagram for the measurement of degradation of Phenolic compound was shown in figure 3.9.

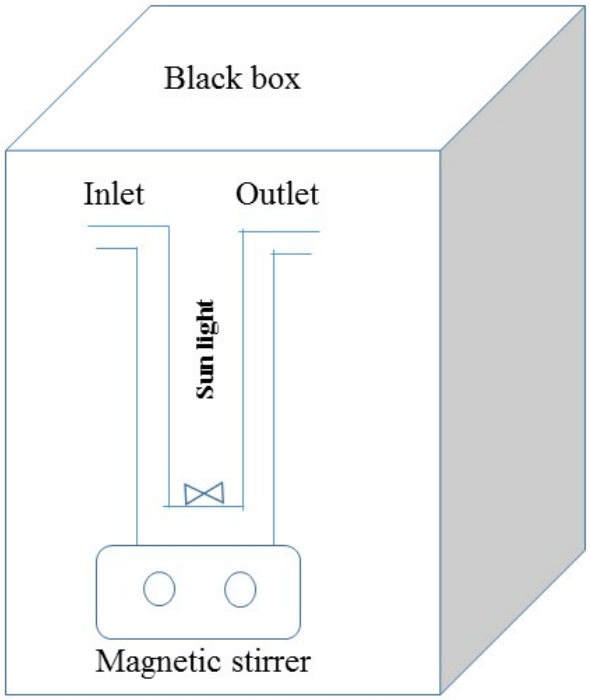

Figure.3.9 Shachamatic diagram of photocatalytic experiment.

3.6 Characterization techniques and instrumentation

In this section, the characterization methods and instruments that have been used in this thesis are described. The prepared nanostructures were characterized by powder X-ray diffraction (XRD), ultraviolet-visible (UV-Vis) spectroscopy, Fourier-transform infrared spectroscopy (FTIR), Field emission scanning electron microscopy, transmission electron microscopy (TEM) and high-resolution transmission electron microscope (HRTEM). The different characterization technique and their mode were listed in table 3.7.

Table 3.7 Characterization Techniques and their Model.

CharacterizationTechniques	Model
X-ray diffractometer	Bruker D8, U.K. Advance equipped
Scanning Electron Microscopy (SEM)	Zeiss EVO 18, USA
High-resolution transmission electron microscopy (HR-TEM)	FEI Mod. No TECHNAI G220.
UV-visible absorption spectroscopy	Jasco V-770, Japan
Photoluminescence Spectroscopy(PL)	SPEX 750M
Infrared IR spectroscopy (FTIR)	IS10 Nicolet, USA
Raman spectroscopy	Renishaw

3.6.1 X-ray Diffraction

X-ray diffraction is a primary non-destructive analytical technique for the determination of the chemical composition and crystallographic structure of the materials. It is also helpful to determine the lattice parameters, lattice defects, lattice strain, crystallite size, and phase of known and unknown materials. It is an electromagnetic wave with a wavelength of the order of one angstrom, and when it is incident upon the sample, diffraction from different atoms takes place. In the crystal, the arrangement of atoms are in a periodic manner, and diffracted x-rays from these atoms take to place an interfere. The present atoms in the crystal formed sharp interference maxima (peaks) with the diffracted waves. This is directly related to the atomic distances. Therefore, the crystal structure of materials can be determined by measuring the distribution of the diffraction pattern. The inter-planer distance can be calculated according to Bragg's law as given below

$$2\,d\,\sin\,\theta\,=\,n\,\lambda \quad \text{---------- (3.6)}$$

Where 'θ' is the incident angle, 'λ' is the wavelength of the x-ray, and 'n' is an integer representing the order of the diffraction. This process is shown schematically in figure 3.9, and the experimental setup shown in figure 3.10.

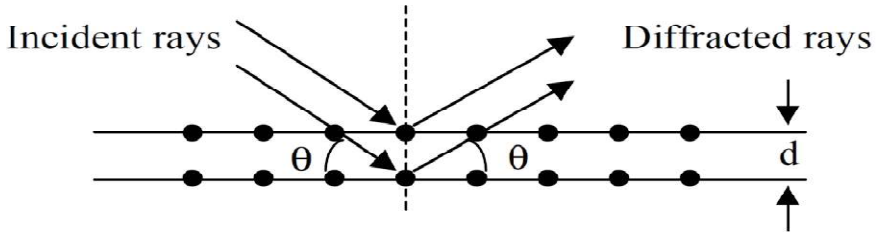

Figure 3.10 Schematic of diffraction of X-rays by a crystal.

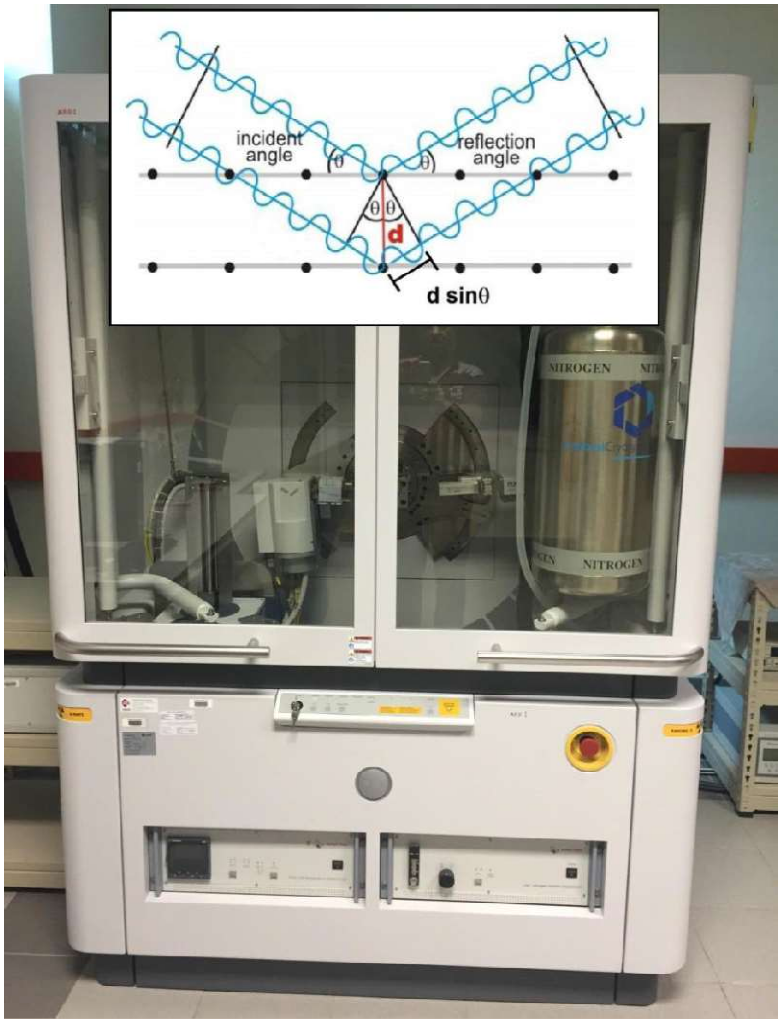

Figure 3.11 X-ray measurement setup.

In our study, the phase evolution and structure of the reduced graphene oxide based nanoceramic composite ZnO nanoparticles (rGO-ZnO) were studied by Bruker D8, U.K. X-ray diffraction experiments were performed using an 18 kW rotating anode (Cuk_{α}) based Rigaku high-resolution X-ray powder diffractometer operating in the Bragg-Brentano geometry and fitted with a graphite monochromator in the diffraction beam. The generator was operated at 40KV and 150mA. The powder samples were placed on a grooved quartz sample holder with the help of glass slide.

The diffraction experiments were applied at a fixed wavelength (λ, $CuK_{\alpha} = 1.54056 A^{O}$) and diffraction angles (2θ) selected were in the range of 10-80^{0} with 5^{0}/min scanning speed.

In our study, the phase evolution and structure of the reduced graphene oxide-based nanoceramic composite ZnO nanoparticles (rGO-ZnO) were studied by Bruker D8, U.K. X-ray diffraction experiments were performed using an 18 kW rotating anode (Cukα) based Rigaku high-resolution X-ray powder diffractometer operating in the Bragg-Brentano geometry and fitted with a graphite monochromator in the diffraction beam. The generator was operated at 40KV and 150mA. The powder samples were placed on a grooved quartz sample holder with the help of the glass slide. The diffraction experiments were applied at a fixed wavelength ((λ, $CuK_{\alpha} = 1.54056 A^{O}$), and diffraction angles (2θ) selected were in the range of 10-80° with 50/min scanning speed.

The crystal size can calculate by Debye Scherer equation:

$$D = \frac{k\lambda}{\beta \cos \theta} \quad \text{---------- (3.7)}$$

where D is the crystallites size of particles, β is the full- width at half maximum (FWHM) obtained by Lorentz fitting of a diffraction line located at angle 2θ , λ is X-ray wavelength and k is a Scherrer constant (0.9), which depends on peak breadth, the crystallite shape, and crystallite size distribution which is dependent on peak breadth, the crystallite shape, and crystallite size distribution (P.Kathirvel et al. 2015).

3.6.2 Strain/Stress behavior of Hexagonal plate by X-ray profile

The interplanar spacing d can be calculated for hexagonal structure (F.K.Shan, B.IKim, et al.2004) such as:

$$d_{hkl}^{\ 2} = \left(\frac{4\left(h^2 + k^2 + hk\right)}{3a^2} + \frac{l^2}{c^2} \right)^{-1} \text{ ---------- (3.8)}$$

Where a and c are the lattice constants, and d_{hkl} is the crystalline plane distance for indices (hkl). Putting the value of *hkl* in equation (3.8) and using the equation(3.7) obtain relation (3.9) for lattice constants a, b for the pane (100) and lattice constants c for the pane (002) and their lattice constant is given by equation (F.K.Shan,B.I. Kim, et al.2004) such as:

$$a = b = \frac{\lambda}{\sqrt{3}\sin\theta} \text{ and } \quad c = \frac{\lambda}{\sin\theta} \text{ ----------(3.9)}$$

Unit cell volume calculated by using the equation (3.10).

$$V = \sqrt{3}a^2 c / 2 \text{ ---------- (3.10)}$$

The dislocation density (δ) was calculated by the following relation (Kathirvel, et al. P 2015)

$$\delta = 1/D^2 \text{ ---------- (3.11)}$$

The microstrain (ε) was calculated by the following formula (P.Kathirvel, et al. 2015).

$$\varepsilon = \beta\cos\theta/4 \text{ ---------- (3.12)}$$

For the materials in the hexagonal crystal structure, the linear stress components can

be described as (P.W. Chi et al.2016)

$$\begin{Bmatrix} \sigma_x \\ \sigma_y \\ \sigma_z \end{Bmatrix} = \begin{Bmatrix} C_{11} & C_{12} & C_{13} \\ C_{12} & C_{11} & C_{13} \\ C_{13} & C_{13} & C_{33} \end{Bmatrix} \begin{Bmatrix} \varepsilon_{xx} \\ \varepsilon_{yy} \\ \varepsilon_{zz} \end{Bmatrix} \text{---------- (3.13)}$$

where C_{ij} is the elastic stiffness constant and ε_{ij} is the linear strain in the *i*th direction as purposed by Maniv S. et al.1982, the stress σ_z is zero in the plane and very close to the edge therefore

$$\varepsilon_{xx} + \varepsilon_{yy} = -\frac{C_{33}\varepsilon_{zz}}{C_{13}} \text{---------- (3.14)}$$

The Stress in the plane can be displayed as

$$\sigma = \sigma_x + \sigma_y = (C_{11} + C_{12})(\varepsilon_{xx} + \varepsilon_{yy}) + 2C_{13}\varepsilon_{zz} \text{---------- (3.15)}$$

Strain along the a-axis (ε_{xx}) calculated by using the formula (Q. GaO et al.2013)

$$\varepsilon_{xx} = \varepsilon_{yy} = \frac{a - a_0}{a_0} \text{---------- (3.16)}$$

Strain (%) along the a-axis (ε_{xx})

$$\varepsilon_{xx} = \varepsilon_{yy} = \frac{a - a_0}{a_0} \times 100 \text{---------- (3.17)}$$

Where 'a' is the lattice parameter of the strained ZnO calculated from X-ray diffraction data.

Combine the eqn. (3.14) & (3.15) obtain eqn. such as:

$$\sigma = \left[2C_{13} - \frac{C_{33}(C_{11} + C_{12})}{C_{13}} \right] \varepsilon_{zz} \text{---------- (3.18)}$$

Strain along the c-axis (ε_{zz}) calculated by using the formula (Q. GaO et al.2013)

$$\varepsilon_{zz} = \frac{c - c_0}{c_0} \text{ ---------- (3.19)}$$

Strain (%) along the c-axis (ε_{zz})

$$\varepsilon_{zz} = \frac{c - c_0}{c_0} \times 100 \text{ ---------- (3.20)}$$

Where c is the lattice parameter of the strained ZnO which can be calculated from X-ray diffraction data.

From the eqn. (3.18) & (3.19) we get

$$\sigma = \left[2C_{13} - \frac{C_{33}(C_{11} + C_{12})}{C_{13}} \right] \left(\frac{c - c}{c_0} \right) \text{ ---------- (3.21)}$$

Substituting the values of the stiffness constant for ZnO in eqn. (3.21) with are C_{11} = C_{33} =210GPa, and C_{13} =105GPa (C.L.Tien, et al.2015, Y.Liu, et al.2013)

So stress σ along the c-axis can be written by the following formula

$$\sigma = 450 \frac{c_0 - c}{c_0} GPa \text{ ---------- (3.22)}$$

To estimate microstrain by Williamson and Hall (W-H) method from the X-ray diffraction pattern Williamson and Hall (T.V.Cuong et al. 2010) proposed a modified Scherer's formula eqn. (3.7) as:

$$\varepsilon = \frac{\beta_{hkl}}{4 \tan \theta} \text{ ---------- (3.23)}$$

$$\beta_{hkl} \cos \theta = \frac{k\lambda}{D} + 4\varepsilon \sin \theta \text{ ---------- (3.24)}$$

For a hexagonal crystal, Young's modulus is given by the following relation (D.Balzar, et al.1993, B.E.Warren, et al.1950).

$$Y_{hkl} = \frac{[h^2 + \frac{(h+2k)^2}{3} + (\frac{al}{c})^2]^2}{s_{11}(h^2 + \frac{(h+2k)^2}{3})^2 + s_{33}(\frac{al}{c})^4 + (2s_{13} + s_{44}(h^2 + \frac{(h+2k)^2}{3})(\frac{al}{c})^2}$$

---------- (3.25)

where 'a' and 'c' are lattice parameters, s_{11},s_{13},s_{33} and s_{44} are the elastic compliances of ZnO.

3.6.3 Scanning Electron Microscopy (SEM)

Scanning electron microscope (SEM), were used for examination of morphology, size, and shape, the elemental composition of the materials. In SEM the electron was emitted from a tungsten cathode. The emitted electron was focused into a very narrow intense beam through two successive condenser lenses. Finally, the narrow beam of the electron was further focused on the sample surface with the help of two pairs of coils. In this primary electrons were emitted and transmit their energy inelasticity to the atomic electrons of the crystal lattice. On the sample, the several scattering processes were taking place. Among them, some electrons managed to leaves the surface and collected by the detector and known as secondary electrons. Finally, the signal was amplified by the photomultiplier tube (PMT) and modulating this signal with the intensity of a cathode ray tube (CRT), and the image of the sample was produced. The good quality image of the sample was produced with a resolution of ~50A°. In our research work, all the samples were used in powder form for the SEM characterization.

3.6.4 Fourier Transform Infra-Red Spectroscopy (FTIR)

The most useful tool for identifying chemicals, organic or inorganic, is FTIR machine. This tool can be used to analyze materials in liquids, solids, and gasses. The characteristic of the chemical bond can be detected from the wavelength of the absorbed light as can be seen in the spectrum. The chemical bonds of the molecule can be determined by studying the infrared absorption spectrum. Each pure compound has a unique FTIR spectrum that called fingerprint. Although the spectrum of organic material is vibrant and detailed, inorganic compounds have simple absorption spectra. For example, ZnO has an absorption band around 400cm^{-1}. Therefore, the unknown materials can be identified by comparison of their spectrum to a library of known compounds. The FTIR machine that used was Fourier transform-infrared (FT-IR) spectrometer (1650: Perkin Elmer, Waltham, MA). The absorption bands between 280 to 400cm^{-1} can be detected by this machine which gives us this ability to identify two of the absorption bands of ZnO Figure 3.12.

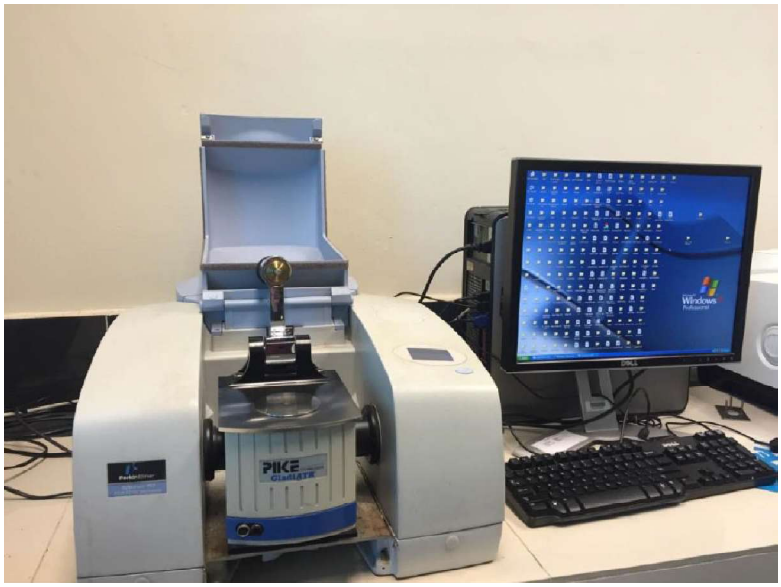

Figure 3.12FTIR measurement setup.

In the FTIR the mostly molecules of samples absorb light in the infrared region of the electromagnetic spectrum which basically represents the bond of the molecules. The FTIR spectrum is measured in the range of 400-4000 cm^{-1}.

3.6.5 Transmission Electron Microscopy (TEM)

Transmission electron microscopy (TEM) is a microscopy technique. In this, the beam of the electron is focused onto an ultra-thin specimen. It is transmitted through the specimen and interacts it. As a result of this interaction, an image is formed. The image is magnified and focused onto an imaging device such as the layer of photographic film or fluorescent screen or is detected using a sensor (e.g., CCD camera). In this work, a Hitachi H-7100 electron microscopy is used in TEM studies. To prepare a sample to use for TEM, a little amount of powders was dispersed in ethanol. The concentration of the suspension should be controlled and depends on the type of material. One or two drops of the solution are poured on the top surface of the copper grid. The copper grid is placed in an oven at 40 ^{0}C for one day.

3.6.6 High resolution transmition electron microscope

HRTEM is a high-resolution technique used to analyze the microstructure of the materials at high resolution. In this tool, the image of the material is produced in two dimensions. The working principle of the HRTEM is similar to a simple microscope. The basic difference in HRTEM and simple microscope are its lenses. In HRTEM, the electromagnetic lenses are used to give the pathway or to guide the beam of electrons while in a simple microscope, the glass lenses are used. In this thesis, one or two drops of the sample were dispersed in water or ethanol for the preparation of the TEM samples, which was followed by drop-casting onto the

carbon-coated copper grid. The copper grid is placed in an oven to evaporate the excess solvent. Finally, the samples were characterized by HRTEM using FEI Mod. No TECHNAI G220.

Figure 3.13 High-resolution transmission electron microscope measurement setup.

3.6.7 Ultraviolet-visible spectroscopy (UV-vis)

Ultraviolet and visible (UV-Vis) is adsorption spectroscopy. It can be used the measurement of the absorption of light when it is passed through from the sample or after reflection from the sample surface. UV-Vis spectra are very helpful for quantitative analysis and sample identification of the materials. It is used to characterize the absorption, transmission, and reflectivity of several of technologically important materials, such as pigments, coatings, windows, and filters. Also, it is used to calculate the optical properties of materials. For example, the absorption spectrum can be used to calculate the optical bandgap. Several methods are used for this, such as the Kubelka-Munk method and first derivative methods as mentioned in literature. In this thesis, Jasco V-770, JapanUV-vis spectrophotometer was used to get the absorption spectra of the rGO-ZnO powder dispersed in ethanol

and measure the spectrum from in the range of 200 to 750nm.

3.6.8 Photoluminescence Spectroscopy (PL)

The photoluminescence spectra are represented by PL. In this spectrum, the light energy, or photons has stimulated the emission of a photon from any matter. The PL system is excited with a 20mW He-Cd laser working at 325nm (3.815eV) and is detected in a black scattering geometry through a photomultiplier and lock-inn amplifier. In our research work, the PL spectrum of all samples was recorded at room temperature using PL experimental set-up (Renishaw System 2000).

3.6.9 Raman Spectroscopy

Raman spectroscopy is the most important technique for carbon-based material characterization. It is a vibrational spectroscopy technique, as similar to infrared spectroscopy. In Raman spectroscopy, a single wavelength of light is used to excite electrons from an energy level into a higher virtual excited state. After excitation, electrons relax to a lower energy level, emitting a photon with an energy corresponding to the energy difference, which is shown in figure 3.14.

In the Rayleigh scattering, the electrons are excited from lower energy state to higher energy state, and after excitation, the electron will relax back to the same energy level that was excited from. In this no difference in energy between the excitation and relaxation. Therefore Rayleigh scattering is not used in Raman spectroscopy. In the Stokes scattering, there is energy deference between excitation and relaxation. It is eqnal to the difference in energy level. Typically, the excitation, in this case, occurs from the ground level where the probability of finding an electron is highest. In Anti-Stokes scattering, an electron relaxing to a lower energy level than its original energy level. The signal produced by Anti Stokes scattering is much smaller

than that for Stokes scattering as the probability of finding an electron in the higher vibrational energy levels is much reduced. Consequently, the Stokes shift is more commonly used to examine the molecular structure.

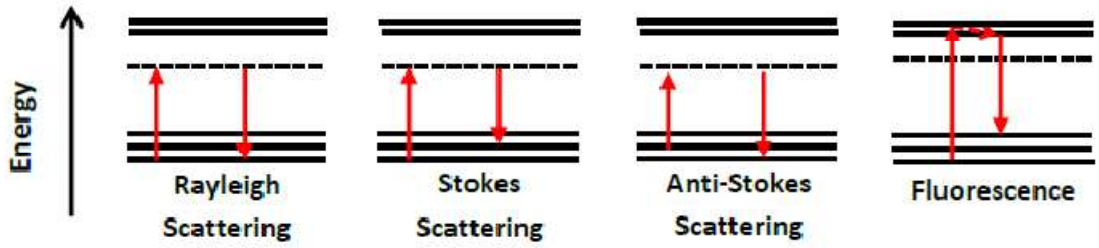

Figure 3.14 Schematic diagram of Rayleigh, stokes and Anti-stokes scattering and fluorescence.

In our research work, The Raman spectra of all rGO-ZnO nanoceramic composites were obtained using a CRM200 confocal Raman Microscope (Renishaw) employing a 532-nm excitation wavelength to confirm the reduction of graphene.

3.6.11Pellets preparation for dielectric behaviour measurement of Hexagonal Plate like ZnO

For dielectric measurement, the synthesize powder of ZnO, ZnO700, ZnO900 and ZnO1100 was consolidated into pellets by using the binder, each with a diameter of 12.36mm thickness of 1.82mm at a pressure of 4-5 tone. The pellet was sintered at 1200^0C in the furnace for 5h and then cooled slowly to room temperature to remove the voids formed during pelletization and silver-coated on the pellets which are used as electrodes. In a typical scheme of pellets preparation shown in figure.3.15.

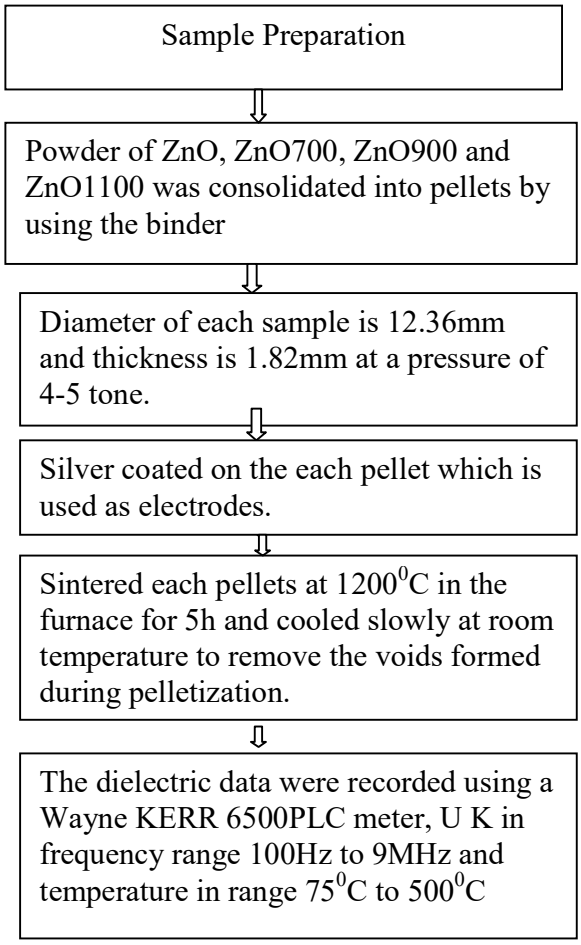

Figure 3.15 Schematic diagrams for Pellets preparation Hexagonal Plate like ZnO.

The dielectric and impedance spectroscopy data were recorded using a Wayne KERR 6500 PLC meter, the U.K in the frequency range of 100Hz to 9MHz and temperatures between 75^{0}C to 500^{0}C. The dielectric properties are an important source of valuable information about conduction processes of materials since it can be used to understand the origin of the dielectric losses, the electrical and dipolar relaxation time and its activation energy(R. Ayouchi et al.2003) that's are mainly determined by their polarizability at a given frequency. The dielectric constant is represented by

$$\varepsilon^* = \varepsilon' - j\varepsilon'' \text{ ---------- (3.26)}$$

The real part of permittivity (ε') represents the polarization of the material and measure amount of energy stored in dielectric due to the applied field while the imaginary part (ε'') represents the energy loss due to the polarization and ionic conductance and describes the dissipated energy in the dielectric field. The value of the real part of dielectric constant (ε') is calculated using formula.

$$\varepsilon' = \frac{C_P t}{A\varepsilon_0} \text{ ---------- (3.27)}$$

Where ε_0 is the permittivity of free space which is equal to 8.85×10^{-12}F/m, t is the thickness of pellet A is the cross-sectional area of pellet and C_p is the capacitance of specimen in Farad.

The imaginary part of dielectric constant (ε'') is calculated using the relation.

$$\varepsilon'' = \varepsilon' \tan\delta \text{ ---------- 3.28)}$$

Where, tanδ is the dielectric loss

The electrical conductivity in the prepared samples is mainly due to the hopping of electrons between the ions distributed randomly over crystallographically equivalent lattice sites (R. Murti et al.2016). The total conductivity is the summation of the band and hopping parts (E.I.Abo, A.M. Ata,et al.2006) and given as:

$$\sigma_{tot} = \sigma_0(T) + \sigma(\omega, T) \text{ ---------- (3.29)}$$

The first term in RHS is the dc conductivity due to the band conduction, which is frequency independent. The second term is the pure ac conductivity due to the hopping process at octahedral sites.

The ac conductivity can be calculated by eqn. (3.29)

$$\sigma_{ac} = \varepsilon^{'}\varepsilon_0 \omega \tan\delta \text{ ---------- (3.30)}$$

where ε' is dielectric constant, ε_0 is the permittivity of free space, ω is frequency,tanδ is the dielectric loss.

Generally, ac conductivity behavior is analyzed using the Josher's power law (R. Punia, et al.2012) and calculated by eqn. (3.31)

$$\sigma(\omega) = \sigma_{dc}\left[1+\left(\frac{\omega}{\omega_H}\right)^n\right] \text{ ---------- (3.31)}$$

Where σ_{dc} dc conductivity is ω_H is crossover frequency separating dc regime (plate region) from the dispersive conduction and n is frequency exponent that lies between 0 and 1. In this equation the conduction mechanism describes with the first term in RHS is the dc conductivity due to band conduction and the second term shows the transport properties of polarons, ions, and electrons (R. Punia,et al.2012).